Adsorption isotherm study of the fractal scaling behavior of vapor-deposited silver films

V. Panella and J. Krim
Physics Department, Northeastern University, Boston, Massachusetts 02115
(Received 26 July 1993; revised manuscript received 19 January 1994)

Adsorption isotherm measurements have been carried out with a quartz microbalance on vapor-deposited silver films, to investigate whether fractal scaling is present. Fractal scaling is in evidence for films deposited at slightly off-normal incidence angles onto substrates held at 77 K. A range of thicknesses has been studied to assess the overall capabilities of adsorption as a probe of dynamic, as well as static, scaling behavior.

PACS number(s): 64.10.+h, 64.60.−i

I. INTRODUCTION

Thin solid film growth, the focus of much recent atomic-scale computer simulation and scaling theory [1], is a topic of long-standing interest on account of its widespread technological application. In order to relate the current wealth of theory to actual physical samples, a knowledge of the films' topography at submicron length scales must be available. The techniques of x-ray reflectivity [2,3], scanning tunneling microscopy (STM) [4,5], electron diffraction [6,7], electron microscopy [8], and adsorption [9] have been employed for the characterization of submicron surface topologies. We focus here on the latter technique of adsorption, and, in particular, on its ability to characterize fractal surface geometries. Specifically, we report liquid-nitrogen data recorded on silver film surfaces which were prepared by near-normal deposition onto substrates held at 80 K. These conditions have previously been reported to result in fractal film surfaces [2]. Our goal is to investigate in more detail the physical origins of this behavior, examining separately the effects of off-normal and low-temperature deposition. A range of silver film thicknesses have been studied, to assess the overall capabilities of adsorption as a probe of dynamic, as well as static scaling behaviors.

After outlining current theory for adsorption on fractal surface, we describe in detail how a quartz-crystal microbalance is utilized to record adsorption data on a vapor-deposited film. We then report our use of this technique to investigate the static and dynamic (film thickness dependent) scaling properties of the vapor-deposited silver films. We conclude with a comparison of experiment and theory, and a discussion of the overall strengths and weaknesses of adsorption as a probe of submicron surface roughness.

II. ADSORPTION ON A FRACTAL SURFACE

A self-similar fractal surface (Fig. 1) preserves its geometric properties when isotropically scaled in all directions. A common method for the determination of its fractal dimension $2<D<3$ involves box counting, whereby the number of boxes of size L needed to cover the surface are described by the relation $N(L)\propto L^{-D}$ [10].

A self-affine surface, characterized by a "static scaling," or "roughness" exponent $0<H<1$ [11], is distinguished from a self-similar fractal by an asymmetry in the scaling behavior perpendicular to the surface (Fig. 1), generally manifested by an absence of surface overhangs [12]. The rms width $\sigma(L)$ of a self-affine surface increases with the horizontal length L sampled according to $\sigma(L)\propto L^{H}$. Self-affine surfaces are characterized by an upper horizontal cutoff to scaling, beyond which the surface width no longer increases. The time evolution of this maximum width during film growth is characterized by the "growth" exponent β, where $\sigma\propto t^{\beta}$ (it is generally assumed that the film thickness h is directly proportional to the deposition time t) [12]. The asymmetric scaling properties of a self-affine surface allow the increments associated with *minimum* height variations perpendicular to the surface, δz, to vary in magnitude from the lateral increments δx over which these variations occur. We note that for actual solid film samples, the ratio $\delta z/\delta x$ is unlikely to exceed 1. The area of a self-affine surface A (as measured by a probe whose size a is less than both δx and δz) is, therefore, unlikely to exceed two times that of a geometrically flat surface A_f, assuming $A/A_f \approx 1+(\delta z/\delta x)^2$.

Adsorption was first suggested as a probe of fractal scaling properties by Pfeifer and Avnir in 1983 [13]. Their "molecular tiling" approach involved measurement of monolayer adsorption quantities for a range of

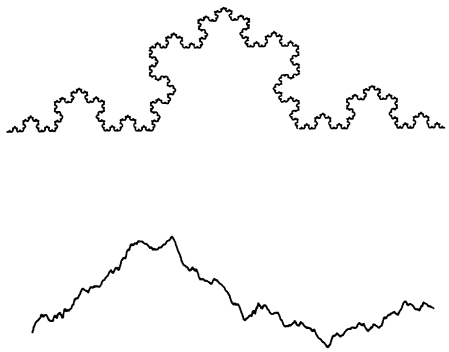

FIG. 1. An example of a self-similar fractal with dimension $D=1.262$ (upper surface) and a self-affine fractal with $H=0.7$ (lower surface).

different adsorbate gases. The number of adsorbate particles N_m with radius a needed to cover a self-similar fractal surface scaled as $N_m \propto a^{-D}$, allowing determination of D. While beautiful in its conception, this approach is limited by a number of experimental constraints [14]. The range of adsorbate diameters available for such a study is greatly restricted, and the potentially porous nature of the surface may inhibit removal of all of the particles of a particular species. A surface which is formed on account of nonequilibrium growth conditions is moreover likely to relax in time, so it is advisable to minimize the length of the data recording session.

Pfeifer *et al.* [9], and also de Gennes [15], suggested that the fractal nature of a surface could also be probed by monitoring the number of particles required to cover the surface as it was progressively smoothed by a thickening adsorbate layer. This approach involves an adaptation of the "Frenkel-Halsey-Hill" (FHH) expression [16] (applicable to films which completely wet planar substrates) [16] to describe the form of an adsorption isotherm on a fractally rough surface:

$$\ln(P/P_0) = -\frac{\alpha}{k_B T \theta^n} . \tag{1}$$

The coefficient α reflects both the substrate-adsorbate and adsorbate-adsorbate van der Waals interactions [17], T is the temperature, θ is the quantity of adsorbed material, and $n = 3/(3-D)$. Numerous authors have argued that the inclusion of adsorbate surface tension effects, neglected in the formulation of Eq. (1), are a necessary aspect of any realistic interpretation of experimental data [18–24]. The discussion is spurred by the fact that relatively little is known on the behavior of surface tension at atomic length scales. Apart from this issue, a consensus exists for the high coverage (thick adsorbate film) forms of $D(n)$ and $H(n)$ [18–23]. If surface tension effects are negligible, then for self-similar [9,15,25],

$$D = 3\left[1 - \frac{1}{n}\right] , \tag{2a}$$

and for self-affine [18,23],

$$n = 3 , \tag{2b}$$

while, if such effects are dominant, then for self-similar [18–23],

$$D = 3 - \frac{1}{n} \tag{2c}$$

and for self-affine [18,23],

$$H = \frac{2}{n+1} \quad (H > 0.5) ; \quad n = 3 \quad (H < 0.5) , \tag{2d}$$

where the value $H = 0.5$, which divides the regimes in Eq. (2d), pertains to nonretarded van der Waals forces.

We focus here on the particular deposition conditions which result in a fractal surface, i.e., a rough surface characterized by an adsorption isotherm of the form of Eq. (1). (Adsorption on a nonfractally rough surface is not described by Eq. (1) [2].)

III. EXPERIMENTAL TECHNIQUE

Adsorption measurements recorded by means of standard volumetric techniques are extremely difficult to carry out on thin-film samples on account of the small surface areas which are typically involved. This difficulty is removed by depositing the film onto the surface of a quartz-crystal microbalance (QCM) [25]. Since a discussion of the use of a QCM for surface-roughness characterization is not available in the literature, we follow with a somewhat detailed discussion of the technique.

An adsorption isotherm is recorded with a QCM by monitoring the pressure dependence of changes in its resonant frequency which result from adsorption on the major faces of the crystal. The crystal vibrates in a transverse-shear mode, and can be driven at resonant frequency with a Pierce oscillator circuit [26]. Changes in its resonant frequency δf_m due to mass loading are proportional to the mass per unit area of the adsorbed film [27],

$$\delta f_m = -\frac{f_0^2 (m/A)}{2.21 \times 10^5} , \tag{3}$$

where f_0 is the resonant frequency in Hz and m/A is the mass per unit area in g/cm^2. One monolayer of nitrogen adsorbed on an 8 MHz resonant crystal with a geometrically flat surface will produce a shift of nearly 10 Hz.

Equation (3) assumes that the electrode surface is geometrically flat. If the surface is instead rough, the area A is still taken as that of a geometrically flat surface. This reflects the fact that the change in frequency due to mass loading is proportional to the total inertial mass of the film which is coupled to the oscillatory motion. Since this paper focuses on adsorbed liquid films which are well coupled to the oscillatory motion of the substrate, we will not address here the case of films which decouple from the substrate [28].

In addition to the massload dependence, the resonant frequency is also dependent, to various degrees, on temperature, pressure, and stresses presented by the deposited or adsorbed film. For example, a 5-MHz crystal will oscillate near 4.995 MHz when cooled to 77 K. The mass sensitivity is not, however, greatly affected by the temperature sensitivity of the oscillator. This can be shown as follows. Equation (3) is based on the relation

$$\frac{\delta f_m}{f_0} = -\frac{m_f}{M_q} , \tag{4}$$

where m_f is the mass of the adsorbed film and M_q is the mass of the quartz crystal. Since neither mass changes upon cooling, the quantity $(\delta f_m / f_0)$ must also remain constant. Dividing Eq. (3) on both sides by f_0, it can be seen that a drop from 5 to 4.995 MHz requires the mass sensitivity constant to drop to 2.078×10^5. Without the adjustment, Eq. (3) will overestimate mass loading at 77 K by 0.1%.

The pressure dependence of the resonance frequency is described by the relation [29]

$$\frac{\delta f_p}{f_0} = -0.72\times10^{-6}\sqrt{\pi\rho_g\eta_g f_0} + (18.35-0.015T)\times10^{-10}P \ . \quad (5)$$

The pressure is in units of torr, the gas viscosity and mass density, η_g and ρ_g, are in cgs units, and the temperature T is in Kelvin. The first term arises from the viscous drag of the gas on the crystal while the second term reflects a change in elastic constants of the quartz due to hydrostatic pressure. The gas pressure contribution to the frequency shift near monolayer completion for a nitrogen film at 77.4 K is close to -2 Hz for an 8-MHz crystal. This term becomes far less important at higher film coverages.

When stresses are presented to the faces of the quartz oscillator, changes in the elastic properties of the quartz produce a shift in the resonant frequency. The magnitude of a stress-induced frequency shift can range from being undetectable to providing a dominant source of frequency shift. Adopting the convention that a positive lateral stress T_f corresponds to film tension, then the frequency shift due to film stress effects is given by [30]

$$\frac{\delta f_s}{f_0} = -2.75\times10^{-11}T_q \ , \quad T_q = -\frac{1}{t_q}\int_0^{t_f} T_f dx \ , \quad (6)$$

where t_q and t_f are the respective quartz crystal and film thicknesses in meters, and T_q is the average lateral stress, in N/m^2, arising from the presence of the film. The lateral stress induced by a liquid-nitrogen monolayer on a flat gold surface electrode has been measured by means of a double oscillator technique [31], and was found to produce a positive frequency shift on the order of 2 Hz. The stress term was observed to be far less significant (with respect to the mass loading term) for higher film coverages.

IV. EXPERIMENTAL RESULTS

The Ag film samples were produced by collimated thermal evaporation of 99.999% pure material at 10^{-7} torr, at 0.3 Å/s onto both faces of optically polished quartz blanks [32], which were held 50 cm above a boat evaporation source. The temperature of the quartz substrate was held at either 80 or 300 K, and the deposition angle was held at either normal, or 5° off-normal incidence. The sample was transferred immediately after deposition, without air exposure, to a tip within the vacuum chamber which could be plunged directly into liquid nitrogen. (Samples prepared at 80 K were warmed to room temperature in the course of this transfer.) After the sample had cooled to 77.4 K, N_2 gas was slowly admitted, and the frequency shift of the oscillator was monitored as a function of pressure, under equilibrium conditions.

Frequency shifts were corrected for pressure effects according to Eq. (5), utilizing gas viscosities determined from the relation [33] $\eta=\eta_c(T/T_c)^{0.965}$, where η_c and T_c are, respectively, the critical viscosity and critical temperature of nitrogen. The frequency shift data presented in Figs. 2–4, therefore, represent both mass loading and nitrogen film stress contributions.

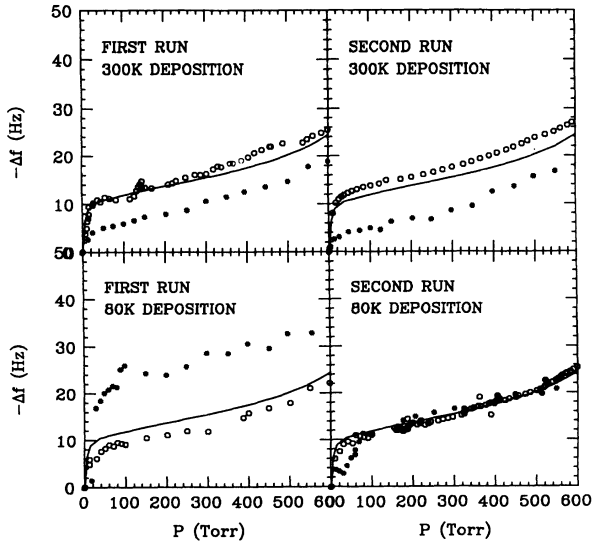

FIG. 2. Low coverage data for N_2 adsorption at 77 K on 1500-Å-thick silver films deposited at 80 and 300 K. Circles denote silver films deposited at normal incidence. Asterisks denote silver films deposited at 5° off-normal incidence. Solid lines denote theoretical prediction for adsorption on a flat silver surface.

Low coverage adsorption data (up to approximately two liquid-nitrogen layers) for 1500-Å-thick silver films deposited at different temperatures (80 and 300 K), and different deposition angles (normal and 5° off-normal incidence) are displayed in Fig. 2. The first and second iso-

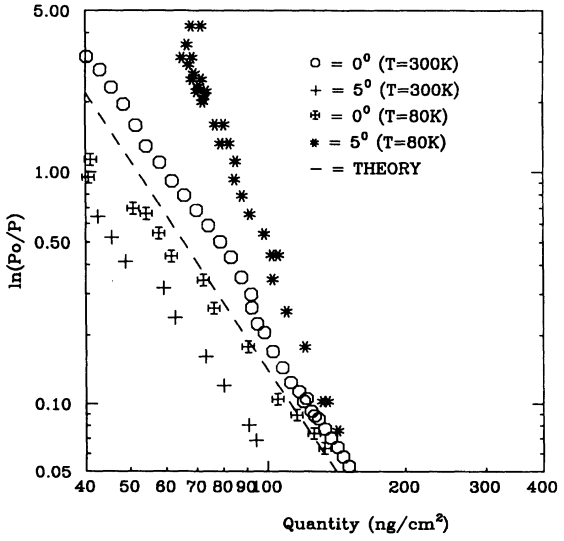

FIG. 3. Thick film data for N_2 adsorption at 77 K on 1000-Å-thick silver films deposited at 80 and 300 K. Adsorption data for both normal (0°) and 5° off-normal silver depositions are presented. The dashed line depicts theory for adsorption on a flat silver surface, and the solid lines are fits to the data. Only the data for the silver film deposited at 80 K and off-normal incidence are characterized by a slope ($n=4.7$), which deviates significantly from that of a flat surface ($n=3$).

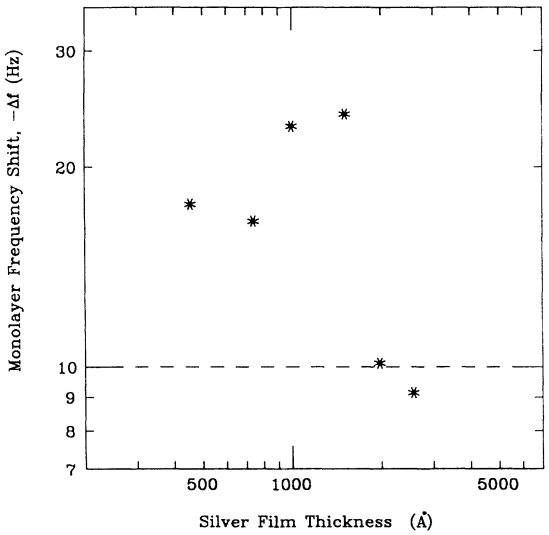

FIG. 4. Frequency shifts associated with N_2 monolayer coverages versus silver film thickness. The silver films were deposited at 80 K and off-normal incidence. The dashed line corresponds to the frequency shift associated with monolayer coverage of a flat silver surface. Larger frequency shifts indicate surface areas which are greater than a geometrically flat plane (see text).

therm recorded on each sample are displayed on the left- and right-hand side of the figure. Solid lines represent the theoretical curve for the mass-loading contribution for nitrogen adsorption on a planar silver surface, with $\alpha = 2.1 \times 10^4$ K Å^3 for N_2/Ag [34]. Data for normal deposition at room temperature fall close to the theory for a planar surface, and no evolution of the data is observed between the first and second measurements. Data for 5° off-normal deposition at room temperature fall slightly below the theoretical curve, presumably on account of an increase in the stress contribution to the frequency shift. No evolution is observed between the first and second data sets recorded on this sample.

Adsorption data recorded on cold-deposited silver films always evolved between the first and second data sets. This effect, which was present for all of the thirty or more cold-deposited films which were studied, was consistent with the formation of nonequilibrium film structures anticipated for the lower substrate deposition temperatures [35–38].

The absolute value of the frequency shifts recorded for normal-incidence deposition exhibited an increase in the second data set, while those recorded for off-normal incidence exhibited a sharp decrease.

The monolayer adsorption data are more susceptible than thick film data to interpretation ambiguities arising on account of the relative contributions of the stress and mass-loading terms. Nonetheless, certain general observations can be made. Ag films deposited at room temperature appear to be more elastic, since no evolution of the data is observed in successive data sets. Ag films deposited at low temperature form structures which evolve in time and may be more brittle than those formed at room temperature. The stress term is opposite that of the mass-loading term, and only the Ag films deposited at *both* off-normal incidence *and* onto a cold substrate exhibit an increase in surface area sufficiently large to overcome the stress effect and be detected by the QCM. That subsequent data sets exhibit no increase in surface area is consistent with a breakdown of the surface structure on account of the first nitrogen adsorption measurement. We note that this apparent structural breakdown was a direct result of the nitrogen adsorption measurement itself, and not the cycling of the sample between 77 K and room temperature.

Figure 3 displays adsorption data for thick nitrogen coverages. The data are plotted as $\ln(P_0/P)$ versus quantity adsorbed on a log-log scale so as to reveal the exponent n in Eq. (1). Since the QCM could not resolve increases in surface area for three of the preparation conditions, it is expected that the thick film adsorption data for these samples should be described by $n=3$. This is indeed the case: Only the cold-deposited, off-normal incidence preparation ($n=4.7$) resulted in data described by an exponent other than $n=3$.

Adsorption data for monolayer and thick nitrogen coverages are displayed in Figs. 4 and 5 for varying (cold-deposited, off-normal incidence) Ag film thicknesses. Low nitrogen coverage data (Fig. 4) show a clear increase in surface area as the silver film thickness increases from 450 to 1500 Å. Above 2000 Å, nitrogen film stress effects evidently overwhelm the mass-loading terms, and the trend reverses itself.

High coverage nitrogen data are described by an exponent $n=3$ for the 450 Å thick Ag film. The exponent $n=4.7$, characteristic of the 1000-Å-thick sample, is within experimental error of that descriptive of the data recorded on both the 1500- and 2000-Å-thick Ag films.

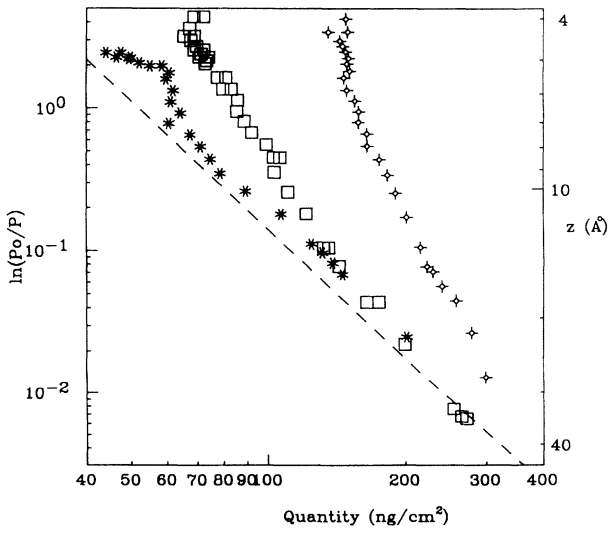

FIG. 5. Thick-film data for N_2 (adsorption at 77 K on 450-Å (asterisks), 1000-Å (squares), and 2000-Å (crosses) thick silver films deposited at 80 K and off-normal incidence. The dashed line depicts theory for adsorption on a flat silver surface, and the solid lines are fits to the data.

V. DISCUSSION

Theoretical models and computer simulations of nonequilibrium vapor deposition onto two-dimensional substrates suggest that $H \approx 0.39$, $\beta \approx 0.26$, if the substrate temperature is low enough to prevent surface diffusion of the deposited film particles upon arrival at the substrate [39–42]. Models which have incorporated diffusion effects have in some cases found no change in the asymptotic behavior of the scaling exponents [43,44], and in other cases have obtained $H = \frac{2}{3}$, $\beta = 0.20$ [45,46].

The fact that the silver films which we study are nonconducting for the first ≈ 200 Å, implies that clusters are forming, and, therefore, surface diffusion is certainly present. They might, therefore, be expected to be characterized by a self-affine roughness exponent H, which falls in the range 0.35–0.70 and a growth exponent $\beta \approx 0.20$–0.26.

According to Eq. (1), three out of four of the deposition conditions which we have studied do not result in fractal growth, since both $n = 3$ *and* no increase in surface area is detected. We note, however, that the QCM technique requires $A/A_f \approx 1.1$ or more in order for the increase in area to be detectable. Taking $A/A_f \approx 1 + (\delta z/\delta x)^2$, this corresponds to a minimum detectable aspect ratio of ≈ 0.3. Self-affine scaling has in fact been reported for silver films deposited at room temperature by the alternate experimental techniques of x-ray reflectivity [47] and STM [48], but the aspect ratios were far less than 0.3.

Adsorption measurements do indicate fractal scaling for the off-normal, cold-deposited samples. Data recorded on these samples clearly indicate increased surface area, and are well described by Eq. (1) with $n = 4.7$. According to Eq. (2), this result is consistent with a self-similar surface whose dimension is either $D = 2.4$ or $D = 2.8$, depending on whether surface-tension effects are included in the analysis. Arguments based on the competing effects of van der Waals forces (which tend to pin the liquid to the walls) and surface-tension effects (which tend to draw the liquid into valleys and crevices) do in fact favor inclusion of surface tension effects, *if the nitrogen film has the same properties as bulk liquid nitrogen.* The latter assumption is, however, far from certain.

Self-affine scaling is apparently ruled out, since the value $H = 2/(n+1) = 0.35$ obtained from Eq. (2b) is not within the equation's range of validity ($H > 0.5$). It has been suggested, however [18], that subleading terms may dominate for some coverage range which precedes the asymptotic range of Eq. (2). If so, the exponent $n = 4.7$ might still be consistent with a self-affine surface. Given the vast theoretical literature predicting self-affine film growth, the fact that the ratio A/A_f does not exceed two, and the fact that x-ray reflectivity measurements show the film densities to be close to bulk Ag, it would be desirable for this theoretical possibility to be further investigated.

Since surface area is not directly related to the rms width of the surface, we are unable to extract an exponent β from the data sets. We note, however, that since the surface area increases with silver film thickness, the "aspect ratio" $\delta z/\delta x$ must also be increasing. This ratio is evidently quite sensitive to the deposition angle and temperature. Such sensitivity may not necessarily be revealed in a numerical simulation of growth, where the magnitude of δz and δx increments is generally fixed in advance.

The technique of adsorption reveals the existence of fractal scaling properties, but provides a highly ambiguous value for H, and no direct information on the value of β. Surface widths (and therefore the scaling parameter β) are more accurately measured by means of x-ray reflectivity [2], so long as the correlation length of the sample remains below that of the x-ray beam (≈ 1 μm). STM, if properly calibrated, can also provide a precise value of σ, and in addition remains viable to much longer length scales (scan heads ranging up to 125 μm are commercially available) [4–5]. The scaling parameter H is, moreover, more accurately measured by means of STM, for lateral length scales exceeding ≈ 100 Å [5]. Finite tip diameters limit resolution below these length scales, so adsorption is the best technique in terms of a truly atomic-scale probe. Despite the various difficulties concerning interpretation of adsorption data, adsorption is the best technique for revealing surface area and porosity of outer surface topology. We conclude that it is powerful not in its own right, but as a tool to be used in conjunction with one of the other experimental probes.

ACKNOWLEDGMENTS

The work has been supported in part by NSF Grant Nos. DMR8657211 and DMR9204022.

[1] For a recent review, see P. Meakin, Phys. Rep. **235**, 189 (1993).
[2] R. Chiarello, V. Panella, J. Krim, and C. Thompson, Phys. Rev. Lett. **67**, 3408 (1991).
[3] H. You, R. P. Chiarello, H. K. Kim, and K. G. Vandevoort, Phys. Rev. Lett. **70**, 2900 (1993).
[4] E. A. Eklund, R. Brouinsma, J. Rudnick, and R. S. Williams, Phys. Rev. Lett. **67**, 1759 (1991).
[5] J. Krim, I. Heyvaert, C. V. Haesendonck, and Y. Bruynseraede, Phys. Rev. Lett. **70**, 57 (1993).
[6] J. Chevrier, V. Le Thanh, R. Buys, and J. Derrien, Europhys. Lett. **16**, 737 (1991).
[7] Y.-L. He, H.-N. Yang, and T.-M. Lu, Phys. Rev. Lett. **69**, 3770 (1992).
[8] D. J. Eaglesham, H.-J. Gossmann, and M. Cerullo, Phys. Rev. Lett. **65**, 1227 (1990).
[9] P. Pfeifer, Y. J. Wu, M. W. Cole, and J. Krim, Phys. Rev. Lett. **62**, 1997 (1989).
[10] T. Vicsek, *Fractal Growth Phenomena* (World Scientific, Singapore, 1989).
[11] J. Krim and J. O. Indekeu, Phys. Rev. E **48**, 1579 (1993).
[12] F. Family and T. Vicsek, J. Phys. A **18**, L75 (1990).
[13] P. Pfeifer and D. Avnir, J. Chem. Phys. **79**, 3558 (1983).
[14] J. M. Drake, P. Levitz, and J. Klafter, Isr. J. Chem. **31**,

135 (1991).
[15] P. G. de Gennes, in *Physics of Disordered Materials,* edited by D. Adler, H. Fritzsche, and S. R. Ovshinsky (Plenum, New York, 1985).
[16] J. Frenkel, *Kinetic Theory of Liquids* (Oxford University Press, London, 1949); G. D. Halsey, J. Chem. Phys. **17**, 520 (1949); T. C. Hill *ibid.* **17**, 590 (1949).
[17] E. Cheng and M. W. Cole, Phys. Rev. B **38**, 987 (1988).
[18] M. Kardar and J. O. Indekeu, Europhys. Lett. **12**, 161 (1990); Phys. Rev. Lett. **65**, 663 (1990).
[19] H. Li and M. Kardar, Phys. Rev. B **42**, 6546 (1990).
[20] P. Pfeifer, J. Kenntner, and M. W. Cole, in *Fundamentals of Adsorption,* edited by A. B. Mersmann and S. E. Sholl (Engineering Foundation, New York, 1991), p. 689.
[21] A. V. Neimark, Pis'ma Zh. Eksp. Teor. Fiz. **51**, 535 (1990) [JETP Lett. **51**, 608 (1990)].
[22] D. Avnir and M. Jaroniec, Langmuir **5**, 1431 (1989); M. Jaroniec, X. Lu, R. Madey, and D. Avnir, J. Chem. Phys. **92**, 7589 (1990).
[23] P. Pfeifer, in *Surface Disordering: Growth, Roughening and Phase Transitions,* edited by R. Jullien, J. Kertesz, P. Meakin, and D. E. Wolf (Nova Science, Commack, 1992).
[24] M. O. Robbins, D. Andelman, and J. F. Joanny, Phys. Rev. A **43**, 4344 (1991).
[25] *Applications of Piezoelectric Quartz Crystal Microbalances,* edited by C. Lu and A. W. Czanderna (Elsevier, Amsterdam, 1984).
[26] J. Krim, Ph.D. thesis, University of Washington, 1984.
[27] C. D. Stockbridge, *Vacuum Microbalance Techniques* (Plenum, New York, 1966), Vol. 5.
[28] J. Krim, D. H. Solina, and R. Chiarello, Phys. Rev. Lett. **66**, 181 (1991).
[29] A. Warner, in *Ultra Micro Weight Determination in Controlled Environments,* edited by S. P. Wolsky and E. J. Zdanuk (Interscience, New York, 1967).
[30] E. P. EerNisse, J. Appl. Phys. **43**, 1330 (1972).
[31] E. T. Watts, Ph.D. thesis, Northeastern University, 1989.
[32] Colorado Crystal Co., Loveland, CO, (303)667-9248.
[33] I. F. Golubev, *Viscosity of Gases and Gas Mixtures* (Keter, Jerusalem, 1970).
[34] S. Rauber, J. R. Klein, M. W. Cole, and L. W. Bruch, Surf. Sci. **123**, 173 (1982).
[35] B. A. Movchan and A. V. Demchishin, Phys. Met. Metallogr. **28**, 83 (1969).
[36] J. A. Thornton, Ann. Rev. Mater. Sci. **7**, 239 (1977).
[37] R. Bruinsma, R. P. U. Karunasiri, and J. Rudnick, *Kinetic of Ordering and Growth at Surfaces* (Plenum, New York, 1990).
[38] *Dynamics of Fractal Surfaces,* edited by F. Family and T. Vicsek (World Scientific, Singapore, 1991).
[39] P. Meakin, P. Ramandal, L. M. Sander, and R. C. Ball, Phys. Rev. A **34**, 5091 (1986).
[40] R. Jullien and P. Meakin, Europhys. Lett. **4**, 1385 (1987).
[41] D. E. Wolf and J. Kertesz, Europhys. Lett. **4**, 651 (1987).
[42] J. M. Kim and J. M. Kosterlitz, Phys. Rev. Lett. **62**, 2289 (1989).
[43] H. Yan, Phys. Rev. Lett. **68**, 3048 (1992).
[44] D. A. Kessler, H. Levine, and L. M. Sander, Phys. Rev. Lett. **69**, 100 (1992).
[45] Z.-W. Lai and S. Das Sarma, Phys. Rev. Lett. **66**, 2348 (1991).
[46] D. E. Wolf and J. Villain, Europhys. Lett. **13**, 389 (1990).
[47] C. Thompson, G. Palazantzas, Y. P. Feng, S. K. Sinha, and J. Krim, Phys. Rev. B **49**, 4902 (1994).
[48] G. Palasantzas and J. Krim (unpublished).